August 1977 LRP 128/77

ION ACOUSTIC TURBULENCE IN A LARGE-VOLUME PLASMA

Y. Kawai, Ch. Hollenstein and M. Guyot

Centre de Recherches en Physique des Plasmas
ECOLE POLYTECHNIQUE FEDERALE DE LAUSANNE

ION ACOUSTIC TURBULENCE IN A LARGE-VOLUME PLASMA

Y. Kawai, Ch. Hollenstein and M. Guyot

Centre de Recherches en Physique des Plasmas
Ecole Polytechnique Fédérale de Lausanne
Lausanne CH-1007, Switzerland

Abstract

Ion acoustic turbulence excited by the current-driven ion acoustic instability in a large-volume plasma is studied experimentally. As the electron drift velocity increases, the fluctuation level of the waves increases and at the same time the peak of the turbulence spectrum shifts to lower frequency. The resulting power spectrum agrees with that predicted by Horton et al.

We measure the effective collision frequency ν of the plasma as a function of electron drift velocity v_d in the presence of the ion acoustic turbulence described above. Below 0.05 v_e approximately, $v_d/v_e \simeq$ constant. Above 0.09 v_e ν/ω_{pe} is proportional to v_d/v_e. It is found that these results can be explained by using the theoretical model of Horton et al., in which the induced ion-wave scattering dominates the turbulence spectrum.

Introduction

A number of experiments[1-5] on ion acoustic turbulence excited by the current-driven ion acoustic instability[6] have been reported. The investigation of the turbulence spectrum itself can be considered to be one of the useful methods of clarifying the nonlinear mechanisms, which dominate the stationary turbulence spectrum. Theoretically various models[7-9] have been proposed by many authors. According to Kadomtsev[7], the increase of the fluctuation level leads to transformation of the wave energy towards the low frequency part of the spectrum due to the induced ion-wave scattering[7], the turbulent spectrum peaks around the cutoff frequency of the instability and is proportional to ω^{-1}. Recently Horton et al.[9] have obtained a modified Kadomtsev spectrum having a lower cutoff, which is derived self-consistently by the induced ion-wave scattering with a quasi-linear growth rate caused by a modification of an electron distribution function due to the feedback effect of the turbulent waves. However this process has not been clarified experimentally so far. Furthermore the turbulence spectrum[1,3,5] observed in steady-state experiments decreases more rapidly with frequency than is predicted theoretically.

As is well known, when the waves become turbulent, the scattering of electrons due to the waves bigins to play an important role in such transport coefficients as electrical resistivity $\rho = m\, \nu / n_e e^2$, where ν is an effective collision frequency can be described[10] quantitatively in terms of the turbulence spectrum. Therefore the measurements of the turbulence spectrum are very important for explaining the effective high collision rate (anomalous resistivity). Experimentally the anomalous resistivity in the plasma has been observed by many investigators[11-16]. However the relationship between the effective collision frequency (anomalous resistivity) and the turbulence spectrum has not been studied in detail, so far.

In this paper, we report the experimental results on the ion acoustic turbulence excited by the current-driven ion acoustic instability in a large-diameter plasma. When the electron drift velocity increases, the ion acoustic wave develops into the turbulent state, in which the induced ion-wave scattering dominates, and the final turbulence spectrum agrees with that predicted by Horton et al. We have also measured the electric fields and the electron drift velocity independently in order to obtain the resistivity of the plasma with the ion acoustic turbulence, and obtained the effective collision frequency as a function of electron drift velocity. The dependence of the effective collision frequency on the electron drift velocity can be explained by using the theoretical results derived by Horton et al.

Experimental Arrangement

The experiments were performed using the plasma box, as shown in Fig. 1. The diameter and length were 70 cm and 35 cm, respectively. The plasma was produced by discharges between the tungsten filaments and the chamber wall, to which were attached permanent magnets. The density and temperature of the electrons were measured by a plane Langmuir probe and an electron energy analyzer, which consisted of the mesh grid G_3 and the collector C. The electron density n_e was varied from 10^9 to 5×10^{10} cm^{-3}, by changing the emission current of the filaments, and was found to be homogeneous throughout the box. The electron temperature was in the range of 1-3 eV. The pressure of the Argon gas was varied from 5×10^{-5} to 5×10^{-4} Torr. The temperature ratio T_e/T_i, which was obtained by determining the dispersion relation of the test ion acoustic waves without instabilities, was found from 10 to 15.

The current-driven ion acoustic instability was excited by imparting a drift velocity to the electrons in the plasma. The drift motion of the electrons was established by applying dc electric fields between the two grids G_1 and G_2 (5 cm in diameter), as shown in Fig. 1. The grids were relatively coarse in order to avoid disturbing the plasma (size of mesh >> Debye length). The potential V_g (0-250 V) was applied to the grid G_1. The unstable waves were detected by the grids and probes, and analyzed by a spectrum analyzer.

The electric field E was observed by measuring the floating potential on the thin two probes (.1 mm in diameter) spaced 1 cm apart, which were placed at the center between the two grids. A directional rotatable probe[15] (5 mm in diameter) located in the plasma between the two grids was used to measure the electron drift velocity v_d. Thus we can determine the electrical resistivity ρ experimentally from the relation $\rho = E/en_e v_d$. On the other hand, $\rho = m\nu/n_e e^2$, so ν is obtained from ρ.

Experimental Results

(1) Ion acoustic instability

We measured the electron drift velocity as a function of grid potential V_g by means of the rotatable Langmuir probe. A typical example is shown in Fig. 2, where $n_e = 10^{10}$ cm^{-3} and $T_e = 2$ eV. This figure shows that initially v_d/v_e increases rapidly with increasing V_g. From linear theory[6], the critical electron drift velocity, above which the instability occurs, is estimated to be about 10 C_s for $T_e/T_i = 15$, so the current-driven ion acoustic instability can be expected in our experiment. Furthermore we can control the growth rate of the instability by changing V_g.

When the grid potential exceeded a critical value (~ 10 V), the low frequency waves were observed in the plasma between the two grids.

Figure 3 shows the power spectrum measured for different V_g, where the distance L between the two grids is 7 cm. When L was shorter, the power spectrum became discrete, as Tanaca et al.[1] have observed. In this case, the phase velocity, which can be estimated by using the relation $\lambda_n = L/n$, were in good agreement with the ion acoustic velocity C_s including the effect of the ion drift motions, where λ_n is the wavelength of the n-th higher harmonics.

In the present experiment, both the mean free path of the electrons and the size of the experimental device are much larger than L, so the plasma is considered to be collisionless. Theory explaining the instability assumes that the electron velocity distribution is a displaced Maxwellian. To measure the electron distribution the energy analyzer was placed just behind the grid G_1 as shown in Fig. 1. The V-1 characteristics for relatively small V_g are shown in Fig. 4, which demonstrates the slope to be exponential so the linear theory of the current-driven ion acoustic instability is applicable. Figure 4 also shows that the plasma potential increases with increasing V_g, which suggests that the electric field may become large with V_g. Unfortunately the electron drift velocity was not obtained from the measurements of the electron distribution because $v_d \ll v_e$. From Fig. 2, Fig. 3 and Fig. 4, we can conclude that the low frequency waves observed here are ion acoustic waves excited by the current-driven ion acoustic instability.

(2) Ion acoustic turbulence

In order to excite the ion acoustic waves with high fluctuation level, the grid potential was increased considerably. We plot both the fluctuation level $\tilde{n}/n_e$ and the frequency f_m at which the spectrum peaked as a function of V_g in Fig. 5, which shows that as V_g is increased the fluctuation level increases, and at the same time the peak of the spectrum shifts to lower frequency. In other words, as the fluctuation level of the ion acoustic wave increases, the wave energy transfers from the high frequencies to the low frequencies, which can be considered as being due to some sonlinear processes.

One of the important aspect in turbulence experiments is a study of the shape of the power spectrum. Assuming the power spectrum $P(\omega) \propto \omega^{-\alpha}$, where α is a constant, we estimated the constant α as a function of V_g. As V_g was increased, α tended to decrease and approached a value of unity around the peak, while α became larger than 1 at high frequencies. Figure 6 is an example of the observed power spectrum for $V_g = 218$ V, where $\tilde{n}/n_e \simeq 0.06$. The shape of the spectrum was independent of the pressure and the distance L (5-15 cm).

When the fluctuation level of the waves becomes large, heating of the electrons can be expected. In fact, we observed the heating up to 20 % by the energy analyzer connected to a sampling circuit.

(3) Anomalous resistivity

As the grid potential is increased, the fluctuation level of the ion acoustic waves rises while above a certain value the electron drift velocity begins to decrease as seen in Fig. 2, indicating the anomalous resistivity. In order to obtain the relationship between the effective collision frequency and the electron drift velocity, we measured both the electric field and the electron drift velocity, in which there was the ion acoustic turbulence described in (2). A typical example for different plasma densities is shown in Fig. 7, where $T_e = 1$ eV, and the pressure was 2×10^{-4} Torr. As seen from Fig. 7, ν/ω_{pe} increases with increasing v_d/v_e and for $v_d/v_e \gtrsim 0.09$, $\nu/\omega_{pe} \propto v_d/v_e$. For $v_d/v_e \lesssim 0.05$, the electron drift velocity seems to be about constant.

The lowest collision frequency in Fig. 7 is still a factor of 30 larger than classical collisions ν_c, as observed elsewhere[15]. In this case, we took the length of the plasma box as a mean free path since the mean free path for electron-neutral collisions was much larger than the size of the plasma.

Discussion and Conclusion

(1) Ion acoustic turbulence

Horton et al. have derived a modified Kadomtsev spectrum from the renormalyzed theory. We obtain the ω -spectrum from the k-spectrum given by the theory, using the relation $P(\omega) \propto k^2 I(k)/d\omega/dk$ as well as the dispersion relation, and plot their spectrum as the dashed curve in Fig. 6. In this case, the theoretical curve was chosen so as to fit the experimental values around the peak of the spectrum. As seen from Fig. 6, the observed power spectrum agrees with that of Horton et al. Thus we can say that in the present experiment induced ion-wave scattering plays an important role in the establishment of the turbulence spectrum. It should also be noted that the observed spectrum deviates from the Kadomtsev spectrum in the high frequencies. This suggests that we can not neglect the effects of the modification of the electron distribution due to the feedback effect of the waves, as Kadomtsev has done.

As seen from Fig. 5, the power spectrum shifts to lower frequency as the electron drift velocity increases. To interpret these results, we calculated the spectrum of Horton et al. for different electron drift velocities. These calculations[17] showed that the peak of the k-spectrum shifts to lower wavenumber with increasing electron drift velocity. Therefore, the shifts of the turbulent spectrum to lower frequency can be considered as being brought about by the induced ion-wave scattering.

(2) Anomalous resistivity

To interpret the experimental results, we calculated the effective collision frequency numerically as a function of electron drift velocity by using that derived by Horton et al. According to them, the effective collision frequency ν is given as follows[9] :

$$\nu = \frac{15\pi}{64}\left(\frac{\pi}{2}\right)^{1/2} \frac{T_e}{T_i} \frac{v_d}{v_e} \omega_{pe} \int_{x_{min}}^{1} dx \left\{ \delta \ln(1/x) - 2(\pi\nu/\omega_{pe})^{1/2} (x^{-1/2} - 1) \right\}$$

where x_{min} is determined by

$$\delta \ln(1/x_{min}) - 2(\pi\nu/\omega_{pe})^{1/2} (x_{min}^{-1/2} - 1) = 0$$

In above equations, $\delta = 1 + \gamma^i / \gamma^e$, where γ^i and γ^e are the damping rate for the ions and the linear growth rate for the electrons, respectively. By solving the above coupled equations, we obtain ν in terms of v_d/v_e. The result for $T_e/T_i = 15$ is shown as the dashed line in Fig. 7. In estimating δ, we neglected the contribution of the high energy tail of the ions, which has been observed in most cases of the turbulent-heating experiments[18]. As seen from Fig. 7, the experimental results agree with the theoretical ones. Parameters in the theory are those during the turbulence. As we have described above, the electrons were heated which may be due to the turbulent heating. Since there were no magnetic fields to confine the ions, it can be assumed in above calculation that the ion temperature is constant during the turbulence.

Here we discuss the theoretical results. The theoretical curve in Fig. 7 demonstrates that (1) $v_d \simeq$ const for $v_d/v_e \lesssim 0.05$ and (2) $\nu / \omega_{pe} \propto v_d/v_e$ for $v_d/v_e \gtrsim 0.09$. Sagdeev and Galeev[10] have derived the relation $\nu \propto v_d$ from the Kadomtsev spectrum which can be understood physically as follows : Since the effective collision frequency depends mainly on the short waves, it is not very sensitive to the detailed shape of the spectrum at small k, so it will not matter much whether the Kadomtsev spectrum or some modification of it is used.

We evaluate the wave energy W in order to obtain the relationship between ν/ω_{pe} and W/n_eT_e. Theoretically we have the following relation: $\nu/\omega_{pe} \simeq (0.30\text{-}0.33)\, W/n_eT_e$. On the other hand, we estimated the wave energy by integrating the power spectrum like Fig. 6 over the frequency and obtained the relation experimentally $\nu/\omega_{pe} \simeq 0.33\, W/n_eT_e$, which agrees with that predicted by the theory. Thus we can conclude from these discussions that the effective high collision frequency (anomalous resistivity) observed here has been caused by the ion acoustic turbulence, in which the induced ion-wave scattering is the dominant process as saturation mechanism of the ion acoustic instability.

In the present experiment, the electric field between the two grids was measured by the thin two probes. When there are high energy electrons in the plasma, the floating potential is determined from the balance between the current due to such a high energy electron and the ion saturation current. Therefore, the existence of the high energy electrons may make the floating potential change locally. However, we have confirmed that the floating potential does not depend on the position without the potential between the two grids.

When the potential is applied to the grid, there may be the possibility that electron beams are produced. However, such an electron beam has not been observed.

We summarize our results as follows : When the electron drift velocity exceeds a critical value predicted by the linear theory, the ion acoustic waves are excited by the current-driven ion acoustic instability in a large-volume plasma. As the electron drift velocity increases, the ion acoustic waves develop into the turbulent state, in which the induced ion-wave scattering dominates the stationary turbulence spectrum. The final turbulence spectrum agrees with that predicted by Horton et al. rather than the Kadomtsev spectrum. We obtained the effective collision frequency caused by such turbulence by measuring the electron drift velocity and the electric field independently. To interpret the experimental results, the effective collision frequency is calculated by using the theory of Horton et al. and compare with the experiment. We find that in the presence of the ion acoustic turbulence, in which the induced ion-wave scattering dominates, the effective collision frequency increase as v_d in large electron drift velocity and v_d seems to be constant in small electron drift velocity.

We would like to thank Professor E.S. Weibel and Dr. J. Vaclavik for fruitful discussions. We wish to acknowledge Dr. Ph. Morgan for reading the manuscript. We also thank Mr. H. Ripper for his technical assistance.

This work was supported by the Swiss National Science Foundation.

References

1) H. Tanaca, A. Hirose and M. Koganei, Phys.Rev. 161 94 (1967).

2) M. Yamada and M. Raether, Phys.Rev.Lett. 32 99 (1974).

3) A. Mase and T. Tsukishima, Phys.Fluids 18 464 (1975).

4) N. Th. Karatzas, A.J. Anastassiadio and K. Papadopoulos, Phys.Rev.Lett. 35 33 (1975).

5) Y. Kawai and M. Tanaka, J.Phys.Soc.Japan 41 1079 (1976).

6) For example, E.A. Jackson, Phys.Fluids 3 786 (1960).

7) B.B. Kadomtsev, Plasma Turbulence (Academic Press, New York, 1965) Chap.4.

8) K. Nishikawa and C.S. Wu, Phys.Rev.Lett. 23 1020 (1969).

9) Duk-In Choi and W. Horton, Jr., Phys.Fluids 17 2048 (1974) ; W. Horton, Jr., Duk-In Choi and R.A. Kock, Phys.Rev. 14A 424 (1976).

10) For example, R.Z. Sagdeev and A.A. Galeev, Nonlinear Plasma Theory, edited by T.M. O'Neil and D.L. Book (Benjamin, New York, 1969) Chap.3.

11) S.D. Fanchenko, B.A. Demidov, N.I. Elagin and D.D. Ryutov, Sov.Phys.JETP 19 137 (1964).

12) B.A. Demidov, N.I. Elagin, D.D. Ryutov and S.S. Fanchenko, Sov.Phys.JETP 21 302 (1965).

13) S.M. Hamberger and M. Friedman, Phys.Rev.Lett. 21 674 (1968) ; S.M. Hamberger and J. Jancarik, Phys.Fluids 15 825 (1972).

14) D. Dimok and E. Mazucato, Phys.Rev.Lett. 20 713 (1968).

15) A. Hirose, I. Alexeff, W.D. Jones, S.T. Kush and K.E. Lonngren, Phys.Rev.Lett. 25 1563 (1970).

16) N.I. Elagin and S.D. Fanchenko, Sov.Phys.JETP 40 674 (1975).

17) M. Guyot and Y. Kawai, to be published.

18) For example, R.D. Bengtson, K.W. Gentle, J. Jancarik, S.S. Medley, P. Nielson and P. Phillips, Phys.Fluids 18 710 (1975).

Figure Captions

Fig. 1 Experimental apparatus, where F are the filaments and L is the probe.

Fig. 2 The electron drift velocity as a function of V_g, where the pressure is 1.8×10^{-4} Torr.

Fig. 3 Typical power spectrum of the observed waves for small grid potential, where (a) $V_g = 9.5$ V, (b) $V_g = 12.5$ V and (c) $V_g = 15$ V. The pressure is 1×10^{-4} Torr.

Fig. 4 The V-I characteristics of the electron energy analyzer with V_g as a parameter.

Fig. 5 The fluctuation level and f_m as a function of V_g where the pressure is 1×10^{-4} Torr.

Fig. 6 The frequency dependence of the power spectrum for $V_g = 218$ V, where $\omega_{pi}/2\Pi \simeq 2.2$ MHz and $v_d/v_e \simeq 0.1$. The dashed curve is the spectrum of Horton et al.

Fig. 7 The effective collision frequency as a function of v_d/v_e at the pressure of 2×10^{-4} Torr, where $T_e = 1$ eV and $L = 10$ cm. The dashed line is the theoretical values.

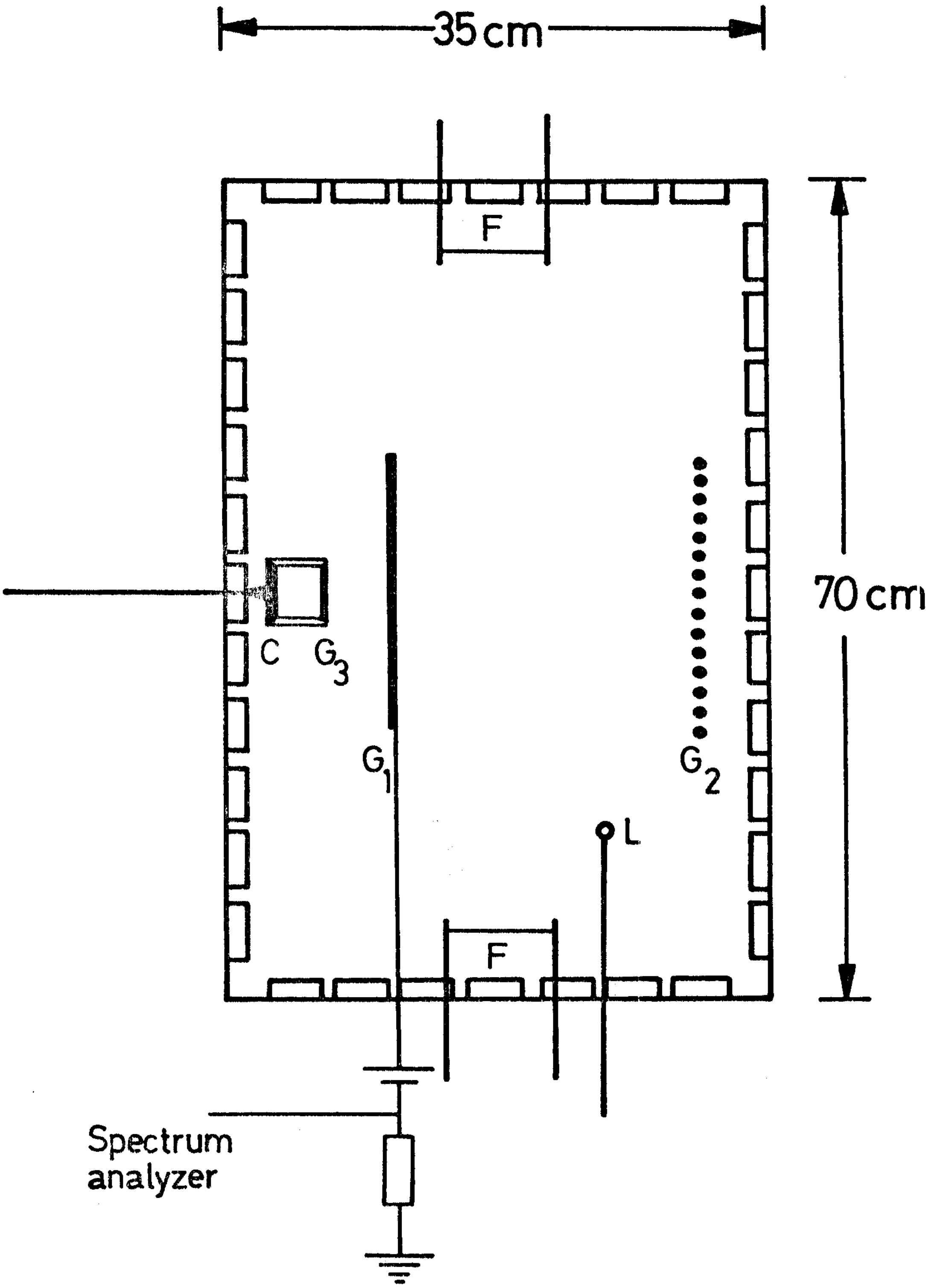

Fig. 1

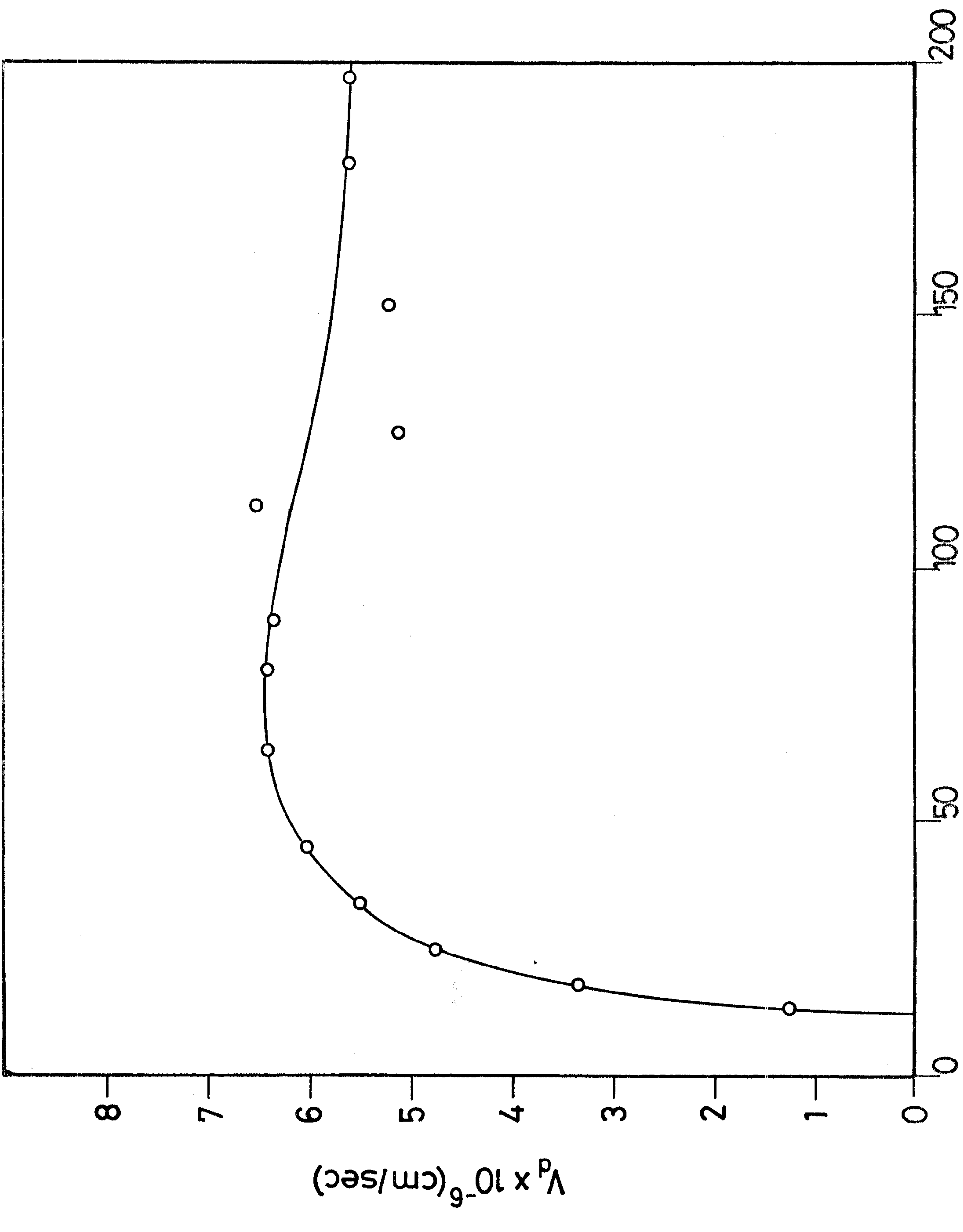

Fig. 2

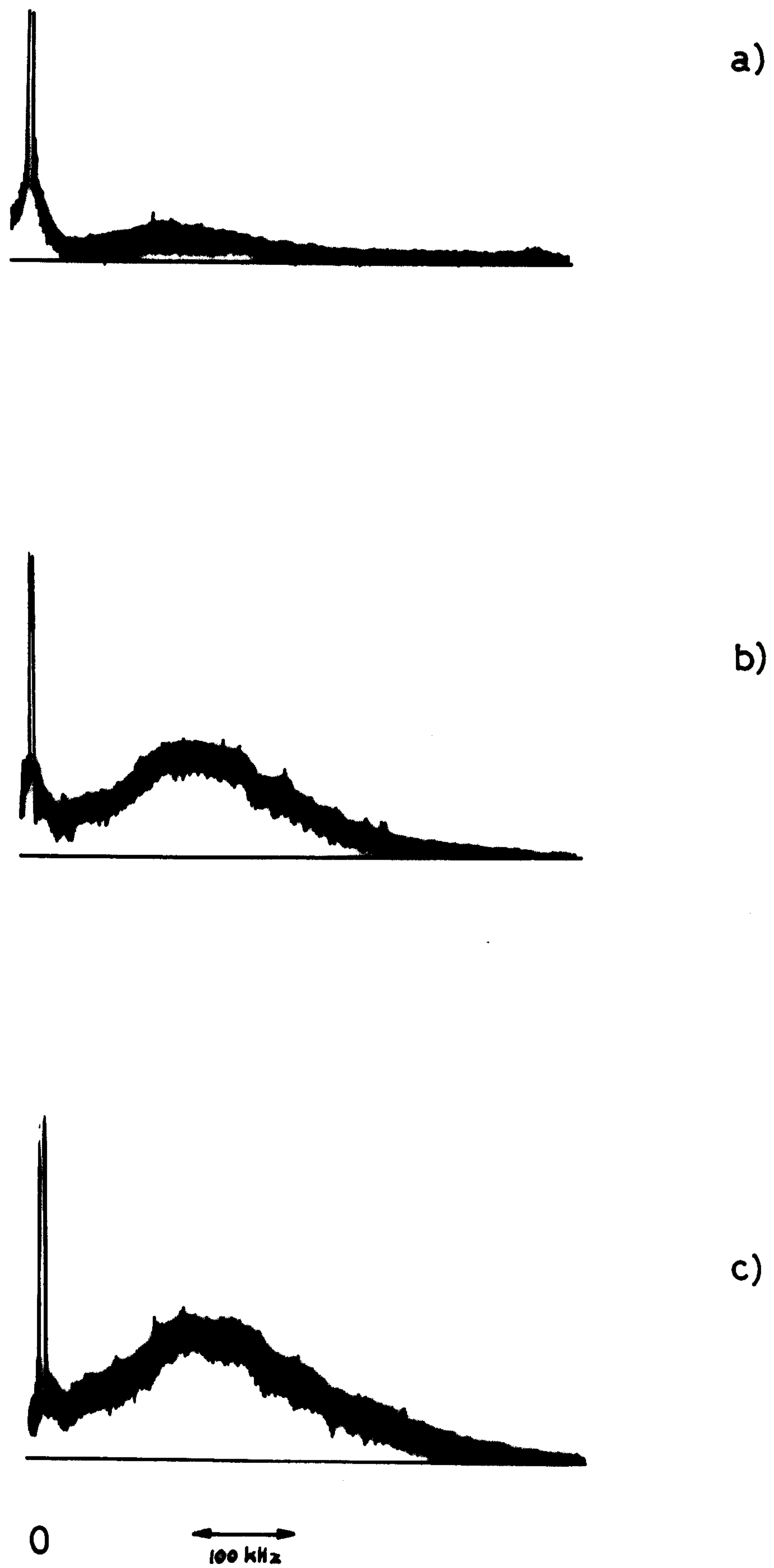

Fig. 3

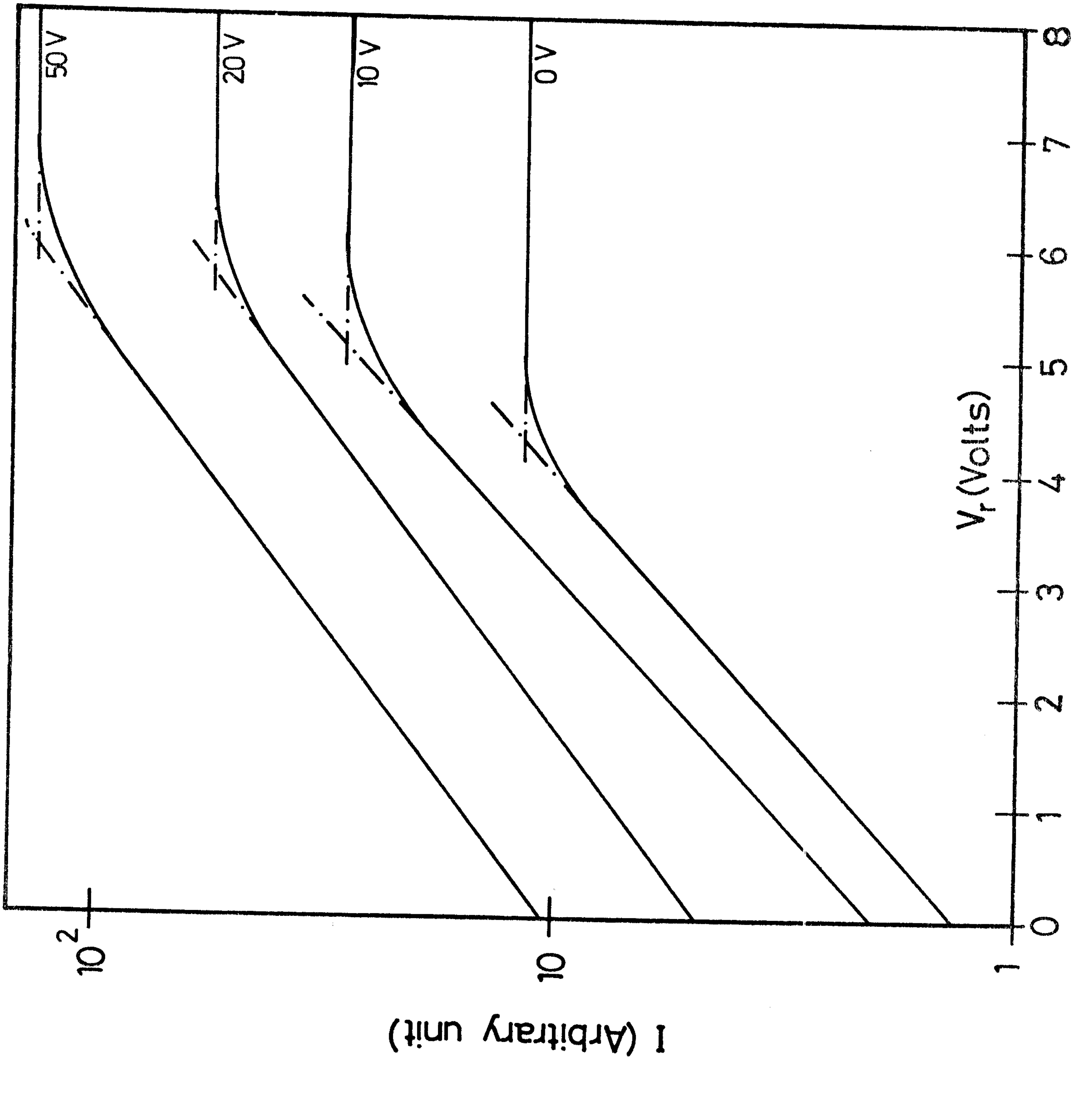

Fig. 4

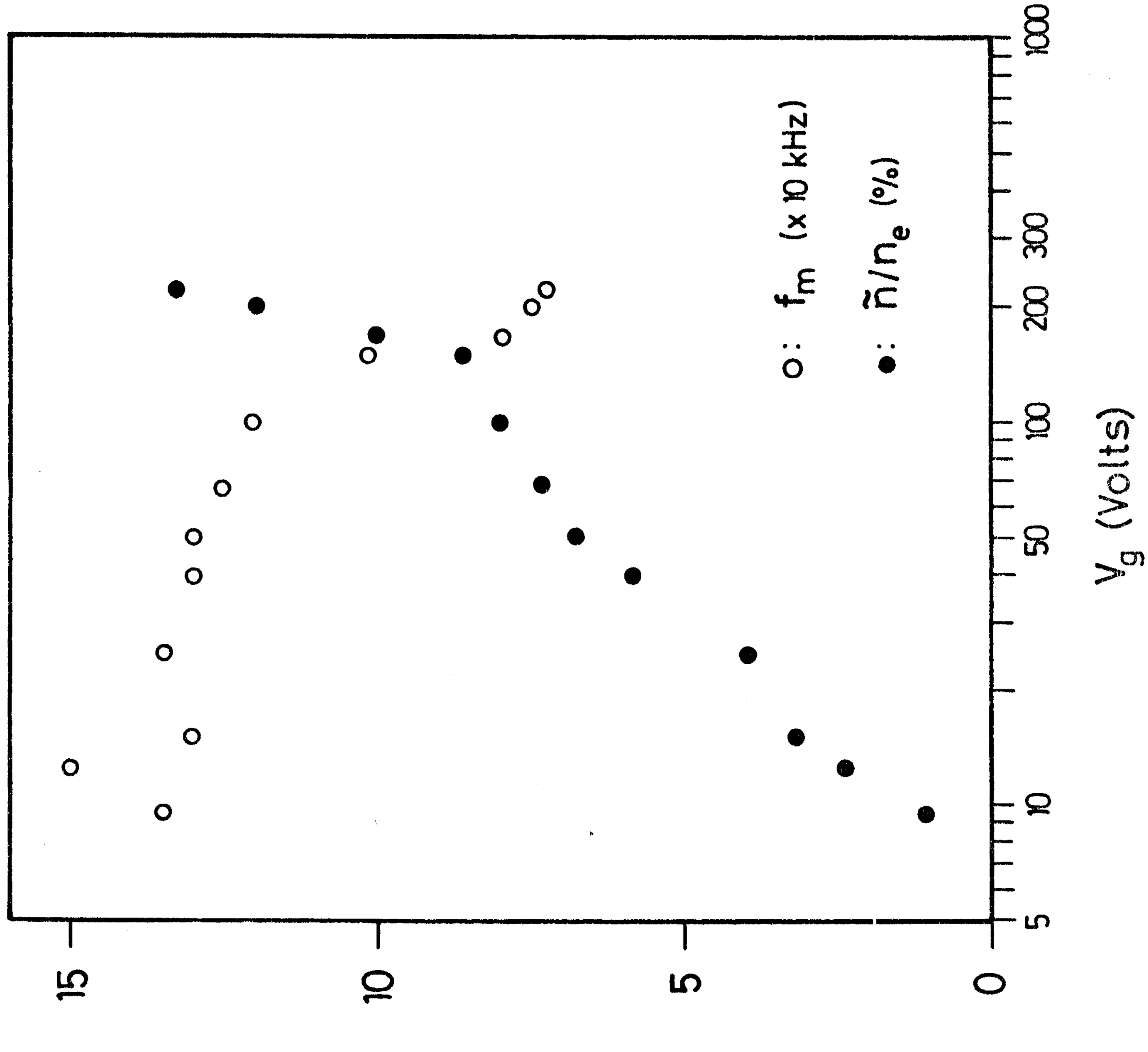

Fig. 5

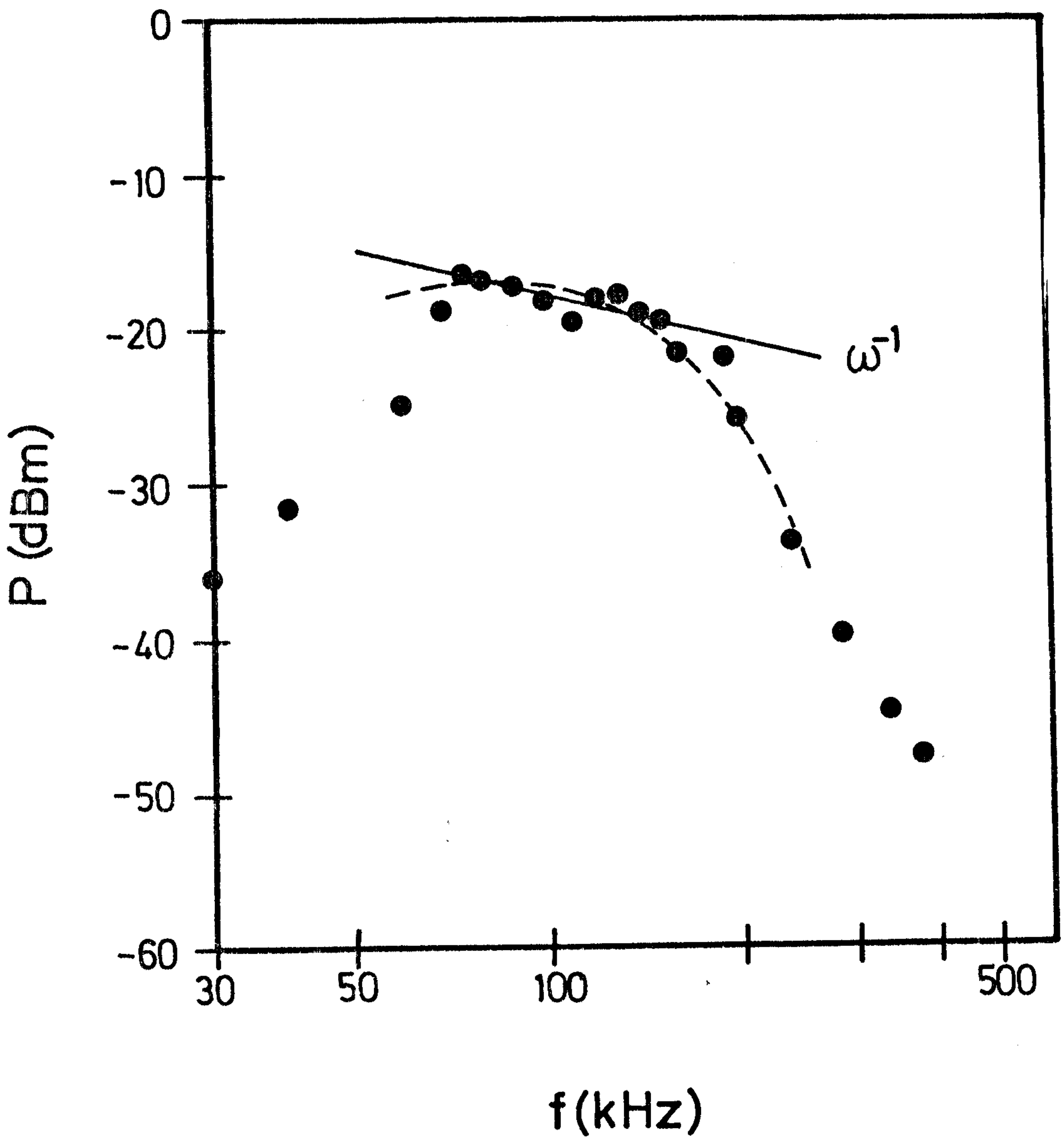

Fig. 6

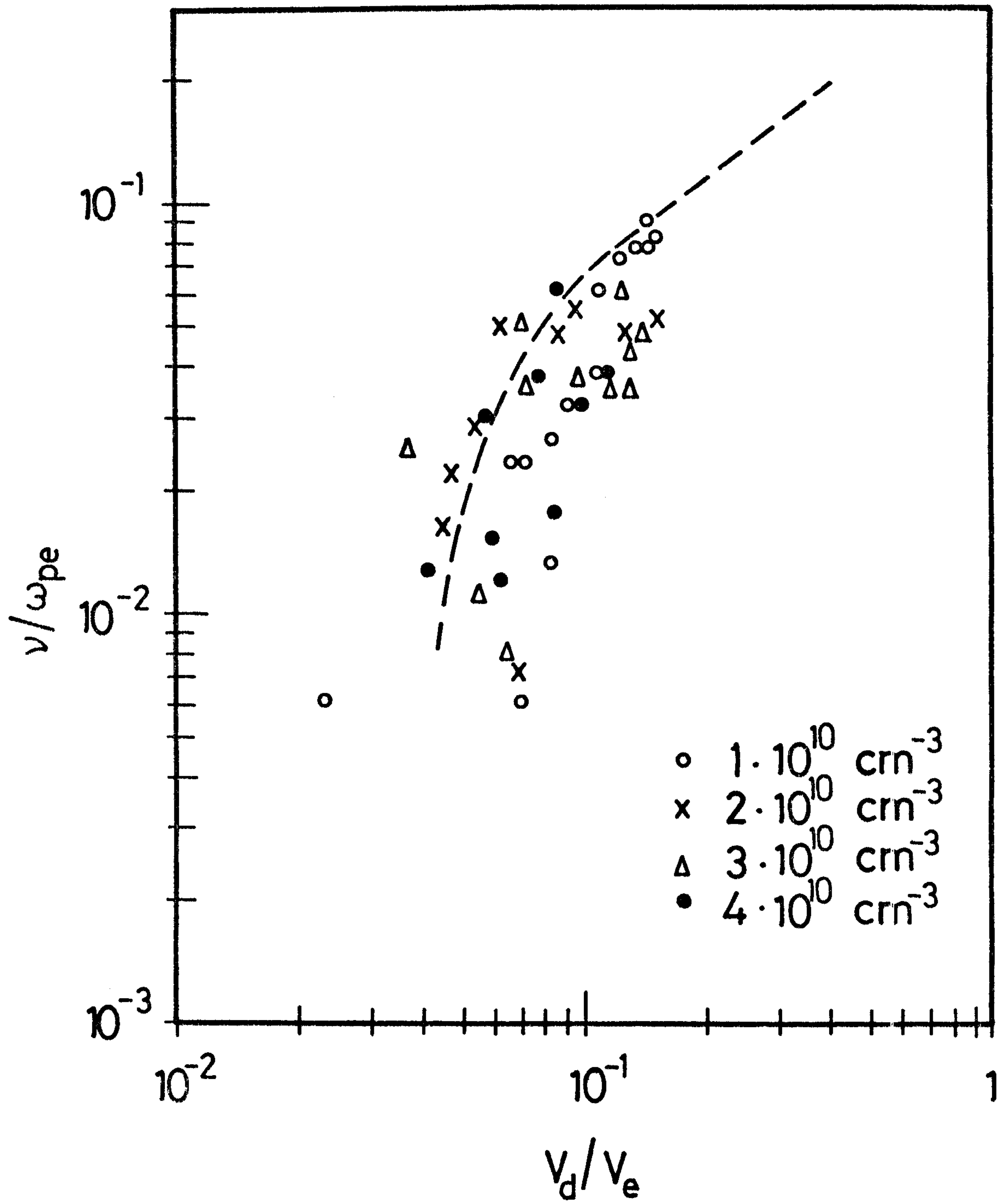
10^{-1}
10^{-2}
10^{-3}
ν/ω_{pe}
10^{-2}
10^{-1}
1
V_d/V_e
$1\cdot10^{10}$ cm^{-3}
$2\cdot10^{10}$ cm^{-3}
$3\cdot10^{10}$ cm^{-3}
$4\cdot10^{10}$ cm^{-3}

Fig. 7